Electrochemical performance of hydrogen evolution reaction of Ni–Mo electrodes obtained by mechanical alloying

L.M. Rodríguez Valdez, I. Estrada Guel, F. Almeraya Calderón, M.A. Neri Flores, A. Martínez Villafañe, **R. Martínez Sánchez**

Abstract

Electro active Ni–Mo electrodes have been prepared by mechanical alloying and pressure-less sintering (1173K) Ni and Mo powders. The electrochemical performance of obtained electrodes has been evaluated in KOH 30% at 343K as a function of the milling time, applied pressure for green compaction as well as the effect conferred by the addition of a process control agent (PCA). Cathodic slope of the best specimen is 279mV/dec. Faster reaction kinetics is observed for the specimens treated with PCA addition. The longer milling time and applied pressure on the specimens the better cathodic response. The activation overpotential, i.e. cathodic-Tafel slopes found at high overvoltages are in the range of 274–481mV/dec, whereas the exchange current density for the hydrogen evolution reaction ranged from 27.3 to 1.4mA/cm2.

1. Introduction

In the last few years, nano-crystalline materials have become an important field of research in materials science due to the unusual properties found in this kind of materials. The extremely small crystals, typically a few nanometers in size, and the large number of grain boundaries, which represent nearly half of the volume of the material, are the origin of the unusual properties [1,2]. In recent dates, these

materials are produced using different techniques; one of them is the mechanical alloying (MA) process. The structure and the properties of several nano-crystalline materials have been discussed by several authors. Electro-catalytic activity is one of the great areas of interest, because the nano-crystalline state can provide a very large number of active sites for reactions [3]. Thus the production of catalyst using novel processes has attracted the attention of world wide research community. Using MA it has been possible to synthesize novel materials with special physical and chemical properties. By the other hand, nickel is a relatively inexpensive and highly active non-noble metal catalyst convenient for developing hydrogen electrodes to be used in alkaline fuel cells [4]. Sturm [5] and Mund et al. [6] found that its catalytic activity was enhanced by additions of transition metals such as titanium, iron and molybdenum. In a previous work, Sebastian et al. [7,8], conducted the Ni–Mo electrochemical evaluation on rapidly densified Ni–Mo electrodes by the spark plasma sintering process (SPS-treated powders).

The present work deals with the production of Ni–Mo electrodes and their subsequent microstructural and electrochemical characterization. The Ni–Mo electrodes were obtained by MA in a high energy ball mill and a subsequent pressure-less sintering (PLS). The electro-catalytic activity of crystalline Ni–Mo alloys is studied to evaluate its hydrogen evolution reaction (HER) in alkaline solution. Additionally, a correlation with their structural characteristics is presented. This work also deals with the milling conditions effect and consolidation pressure as reflected in the electrochemical properties.

2. Experimental details

2.1. Powder synthesis and sintering

Ni (99.9% pure, −200 mesh in size) and Mo (99.5%, −200 mesh) powders were used as raw materials. Nominal composition was set to Ni-53 at% Mo, amounts which correspond to the intermetallic compound Ni–Mo. Simoloyer mill was used to accomplish MA operation of the powder mixtures. The milling time intervals were set to 9, 18 and 36h based on previous results [9, 10]. The milling media to powder weight ratio was 20 to 1. The sample weight was 50g. Methanol was used as process control agent (PCA) for specific experiments, additionally, some other experiments were performed with no PCA addition. Devices and milling media used were made from stainless steel (SS). Vacuum atmosphere was maintained along milling. The as-milled products were characterized using several techniques. X-ray diffraction (XRD) through a Diffractometer D-5000 Siemens with Cu–Kα(λ=0.154nm) radiation and graphite monochromator. XRD data were collected with a step mode of 0.05° with a collection time of 10s/step. Scanning electron microscopy (SEM) was conducted with a JEOL JSM 5800 LV supplied with EDS spectrometer.

2.2. Electrochemical tests

For electrochemical measurements the powders were compacted by cold uniaxial pressing at 945 and 1250MPa. Green consolidated samples were PLS at 1173K during 5h under vacuum atmosphere. The characterization of the consolidated samples was carried-out by above described techniques. A commercial potenciostat/galvanostat/ZRA controlled by a personal computer was used to carry-

out electrochemical tests. Electrochemical experiments were performed in a typical three electrode system. The working electrode (W, anode) of the electrochemical cell was a mechanical alloyed and sintered Ni–Mo alloy, which was previously coupled to a Cu wire by Ag epoxy. Specimens of various processing conditions were mounted in epoxy resin as to expose a polish face of 6.3mmφ directly with test solution. The electrolyte (testing solution) was KOH 30% w/w high grade solution, which was kept stirred and at 343K during all electrochemical analysis to avoid concentration polarization drawbacks. The testing solution was nitrogen-bubbled at least 1h before and during the measurements. The counter electrode (CE, cathode) was pure Pt wire and the reference electrode was an Ag^{+}/AgCl electrode. The electrochemical measurements were carried-out by potentiodynamic polarization curves using ± 1000mV interval at a scanning rate of 10mV/min.

3. Results and discussion

3.1. Mechanical alloying

Amorphization of the Ni-53 at% Mo powder under Ar atmosphere is followed from the XRD analysis conducted at different milling times. The corresponding XRD patterns are collected in Fig. 1(a,b). The as-mixed XRD pattern corresponds to a Ni and Mo mixture (not milled) powder. After 9h of milling most Ni peaks disappeared whereas those remaining turned broad and shortened. Moreover, judging from the slight displacement of the main Ni diffraction peak (111) to lower 2θ angles as the milling time increases (18h), the formation of a solid solution might be inferred. The XRD pattern obtained after 36h, suggests that preferential and partial amorphization has occurred as deduced from the presence of a broad diffraction XRD background

in the Ni peaks position, as well as the remaining Mo peaks. The 36h XRD pattern suggests the coexistence of an amorphous-like phase with un-reacted and nano-crystalline Mo powder. Apparently, for Ni–Mo alloys prepared by MA, it appears that Ni is an element prone to amorphize with Mo, whereas the opposite is not necessarily true [2]. The amorphous phase formation starts with the solution of one element into the matrix of the other. This solid dissolution increases defects density in the host nickel matrix, finally inducing the amorphous-like phase formation. In all XRD patterns it is clear that the typical diffraction peaks ($2\theta \cong 40°$) corresponding to Mo (110) suffered shortening and broadening without position shifting. This might indicate that Mo is not dissolving Ni or Fe (released from the milling media wear). At a first approach, this result would had been expected considering the non-solubility of both nickel and iron in molybdenum, as reported in the phase diagrams [11,12].

3.2. Electrochemical characterization

Recently, far from equilibrium structures obtained by MA had received much attention; in nano-crystalline alloys, the large amount of grain boundaries and the intergrain disorder often discussed in the literature, may be an important source of active sites [1–3]. It has been reported before that the electro-catalytic active phase is attributed to the presence of over saturated and nanocrystalline FCC solid solution of Mo into Ni [1], however the basic reasons for having such good properties are, in fact, still unknown. By the other hand, it has also been reported that potentiodynamic polarization analysis confirmed that microstructural factors such as metastability, galvanic couples and particle size distribution on these electrodes are required for effective hydrogen gas production [2,3,7,8]. In spite of this, there are no reports

concerning electrochemical studies carried-out in structures close to thermodynamic equilibrium. Fig. 2 shows the cathodic polarization curves evaluated from the Ni–Mo samples after PLS at 1173K. The corresponding

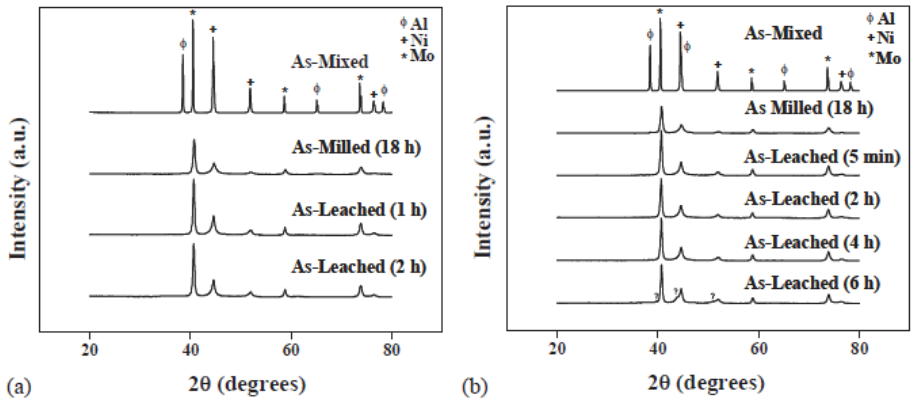

Fig. 1. XRD spectra for Ni–Mo mixtures milled for different times under vacuum atmosphere: (a) PCA addition, (b) No-PCA addition.

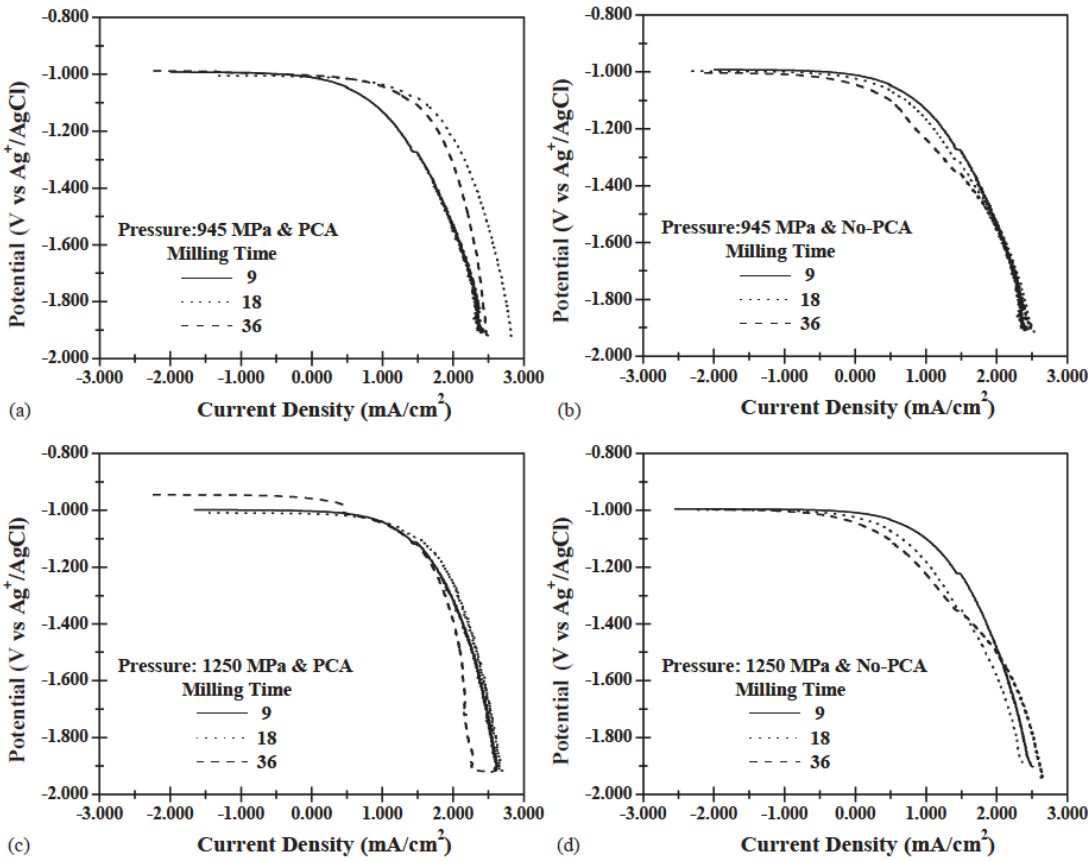

Fig. 2. Cathodic polarization curves of sintered samples at 1173 K, from which Tafel B_c slope was estimated: (a),(b) cold compacted at 945 MPa and (c),(d) cold compacted at 1250 MPa.

electrochemical parameters are included in Table 1. From Fig. 2 and Table 1 it is evident the milling time effect on the electrochemical parameter as well as the compaction pressure effect of products. The reported open circuit potential E_o=E_{corr} (i.e. the E_{ocp} potential of the electrode with respect to the solution) reached a steady state in <20min after dipping the Ni–Mo electrodes, into the alkaline solution. E_o values were found to be fairly

Table 1
Electrochemical parameters of Ni–Mo alloys obtained by MA and PLS at 1173 K. Testing solution was KOH 30 wt%, at 343 K

Milling time (h)	Pressure (MPa.)	PCA addition	E_o vs Ag^+/AgCl (mV)	B_c mV/decade	i_{corr} (mA/cm^2)
9	945	Yes	−913	481	10.72
9	945	No	−906	321	3.89
9	1250	Yes	−917	349	10.81
9	1250	No	−894	289	4.79
18	945	Yes	−916	389	27.29
18	945	No	−909	331	3.15
18	1250	Yes	−911	297	10.11
18	1250	No	−874	327	2.73
36	945	Yes	−914	407	18.74
36	945	No	−899	274	1.37
36	1250	Yes	−916	368	10.46
36	1250	No	−945	279	1.54

E_o: Open-circuit potential, B_c: cathodic slope, i_{corr}: corrosion current density.

reproducible on each treated specimens. Before being polarized the specimens shortly adopted an E_o stable in the negative region, turning even more negative after testing.

The electrode potential was observed to vary from −874 to a minimum of −945mV. In general, it was observed that E_o values were lower for the samples prepared without PCA addition. The absolute value of these negative data is an indirect indication of how extraordinary active these electrodes behave at 343K in such testing environment. Comparable testing values (vs.Ag^+/AgCl) have been

reported before [1–3,7,8].

The dE/d(logi) slopes (Bc) for the samples milled with no PCA additions (b) and (d) are quite flat. Additionally, in the no-PCA specimens Bc turns lineal versus the milling time increase (Fig. 2b and d), revealing the milling condition effect on the electrochemical process, as it was reported before [2,3]. Theoretically, the smaller Bc the better electrode for catalyzing HER [1–3,7,8]. From Table 1 it is observed that the alloys prepared with no additions of PCA present the lower Bc values under the study conditions. The Bc values reported in this work are close to those Bc reported before [1–3,6,7]. This processing route, milling and sintering conditions used in this work, offer a long term life electro-catalyst.

In a number of the above mentioned papers [1–3,7,8] two Tafel slopes (Bc and Ba) are reported. The Bc values reported in the present work are close to those high Bc reported before for several authors. However, Janik-Czachor et al. [3] previously commented about this case that, small slopes of the order of ~60mV have been calculated from the low overpotential parts of polarization curves. This procedure, however, might be misleading since a well-defined linear E vs. logi dependence can only be measured for overvoltages larger than 100mV. For lower values, the E vs. logi curves are steeper because of the overlap with the reverse reaction, which is also potential dependent [3].

The electrochemical reaction kinetics is faster in samples milled with PCA additions. On the other hand, it was observed that all milling times used in the present work, the effect is particularly large at low overvoltages where the current density is almost one order of magnitude higher than that of samples milled with no

PCA additions, see Fig. 2 and Table 1. The PCA effect is more evident than the pressure employed during cold-consolidation in the electrocatalytic activity. A difference on the slope of these curves, points out not only to significant changes on the oxidation behavior of the specimens but also to substantial variation of their ability to catalyze HER.

4. Conclusions

Milling conditions as conducted in this work have an important effect on the electro catalytic properties of studied Ni–Mo electrodes. Samples prepared under PCA action undergo faster reaction kinetics than those prepared with no additions. Cathodic slope of the best specimen was 279mV/dec.

The longer milling time and applied pressure on the specimens the better cathodic response.

Acknowledgements

This work was supported by CONACYT (J32620-U). FAC and RMS acknowledge to CONACYT-SNI. IEG acknowledges CONACYT scholarship. Thanks to A. Reyes-Rojas, V. Orozco-Carmona, J. Lugo-Cuevas and G. Vazquez-Olvera for technical assistance.

References

[1] Schulz R, Huot JY, Tradeu ML, Dignard-Bailey L, Yan ZH. J Mater Res 1994;9(11):2998.

[2] Portnov VK, Oleszak D, Fadeeva VI, Matyja H. Proceedings of the Rapidly Quenched and Metastable Materials, 25–30 August, 1996, Bratislava, Slovakia.

[3] Kedzierzawski P, Oleszak D, Mjanik-Czachor. Mater Sci Eng A 2001; 300A : 105.

[4] Kenjo T. J ElectrochemSoc 1985;132(2):383.

[5] Von SturmF. In: McIntyre JDE, Srinivasan S, Will FG, editors. Proceedings of the Symposium on Electrode Materials and Processes for Energy Conversion and Storage, Princeton, New Jersey: The Electrochemical Society, Softbound Proceeding Series; 1977. p. 247.

[6] K. Mund, G. Richter, St.ur.m. VonJ. Electrochem Soc, 124 (1) (1977), p.

[7] S.D. De la Torre, D. Oleszak, A. Kakitsuji, K. Miyamoto, H. Miyamoto, R. Martínez-Sánchez, F. Almeraya-Calderón, A. Martínez-Villafañe, D. Ríos-JaraMater Sci Eng A, A276 (2000), p. 226

[8] S.D. De la Torre, D. Oleszak, F. Almeraya-Calderón, A. Martínez-Villafañe, R. Martínez-Sánchez, D. Ríos-Jara, H. MiyamotoJ Metastable Nanocryst Mater, 8 (2001), p. 855

[9] R. Martínez-Sánchez, S. Díaz de la Torre, F. Espinosa-Magaña, L. Bejar-Gómez, J.G. Cabañas-MorenoJ Metastable Nanocryst Mater, 10 (2001), p. 2001

[10] R. Martínez-Sánchez, I. Estrada-Guel, D. Jaramillo-Vigueras, S.D. de la Torre, C. Gaona-Tiburcio, J. Guerrero-PazJ Metastable Nanocryst Mater, 13 (2001), p. 135

[11] Singleton MF, Nash P. Ni–Mo system. In: Massaslki TB, editor. Binary alloy phase diagram. USA: ASM International; 1992. p. 2635.

[12] Fernandez Guillermet A, Mo–Fe system. In: Massaslki TB, editor.

Binary alloy phase diagram. ASM International; 1992. p. 2635.